ELSEVIER

Chemical Engineering Journal 135S (2008) S276–S279

Chemical Engineering Journal

www.elsevier.com/locate/cej

Electronically programmable membranes for improved biomolecule handling in micro-compartments on-chip

S. Chemnitz, U. Tangen, P.F. Wagler*, T. Maeke, J.S. McCaskill

Ruhr-University Bochum, BioMIP, BioMedicineCenter, Otto-Hahn-Str. 15, 44227 Dortmund; Germany

Abstract

This work is focused on the design, fabrication and application of microfluidic compartments containing on-line programmable membranes. Both electroosmotic and electrophoretic effects are used to control the transport, pre-concentration and transfer of DNA within a microfluidic network. The experimental platform is based on a hybrid microfluidic chip containing a silicon substrate with integrated gold electrodes and a plastic fluidic layer, which consists of a network of channels and microreactor compartments. The PDMS microfluidic moulds were designed and pre-fabricated from an SU-8 master with standard lithography methods [1].

Keywords: Microfluidic; Electroosmotic flow; Microreactor; DNA; Artificial membrane

1. Experimental setup

An overall experimental setup based on a laser-scanning microscope (Olympus BX51) and a biochip environment – the field programmable fluid array (FPFA) – is shown in Fig. 1. It contains also high performance pumps controlled via serial-interfaces, an EMCCD-camera for image acquisition (Andor DV885JCS-VP), motorized stepper xy- and z-stages (Prior, Physik Instrumente GmbH & Co. KG), different diode pumped solid state laser sources (Coherent 488 nm, 200 mW and Lasos 639 nm, 25 mW) as well as an optional confocal scanner unit. All components are managed by a custom designed and built controller board and a Linux host-computer.

An adapter frame as shown in the left image of Fig. 1 allows the build-up of temperature-gradients on-chip as well as two different types of FPFA. Major effort was spent to allow high-precision objectives, which usually have very small working distances. A small PCB with a connector provides control of the field programmable gate array (FPGA) and/or the electrodes on the FPFA. The adapter is modular and allows mounting inside a 80 cm × 80 cm cartridge for standard z-stage devices as well as in an optical slide and a special minimum-size cartridge. The thermal capacity of the carrier is minimized and supports a quick temperature cycling and cooling below zero °C. Two temperature sensors are integrated into the carrier, additional ones can be attached.

The microfluidic design of an electronic regulated membrane is shown in Fig. 2 and based on a modified "H-structure" [1,2] with vertical source and drain channels merging to a single outlet. Both vertical channels are connected by a horizontal oriented and very shallow transfer channel (structure height 1.1 μm, width 40 μm) well positioned at two pairs of electrodes (see also microscope image in Fig. 2) at the bottom and the circular detection/reaction chamber (height 35 μm by 60 μm diameter). Both vertical channels outputs merge into one output channel to get an extremely stable fluidic behaviour (passive control). Microfluidic channels and compartments were micro-moulded in PDMS (polydimethylsiloxane, Sylgard 184) after the pre-fabrication of an SU-8 master using standard soft-lithography methods. The first design of this structure and proof-of-principle experiments for laser-driven fluorescence detection of biomolecule concentration and routing was presented in a recent work [3]. All hydrodynamic resistances of the entire fluidic network have been calculated. The result is a driving electroosmotic flow (EOF) in combination with pressure flow along the horizontal channel.

The hybrid microfluidic chip is equipped with 96 gold-electrodes (size typically 20 μm × 40 μm or 40 μm × 40 μm) and a programmable logic device (FPGA, Spartan XCS20CSP144 Xilinx) that serves as the driver for the electrodes via standard output driver voltages, entailing a digital 3.3 V signal level. With the three states provided (3.3, 0 V and tristate) fast cycling allows us to emulate effectively arbitrary

* Corresponding author. Tel.: +49 231 9742 6423; fax: +49 231 9742 6426.
E-mail address: patrick.wagler@rub.de (P.F. Wagler).

1385-8947/$ – see front matter © 2007 Elsevier B.V. All rights reserved.
doi:10.1016/j.cej.2007.07.061

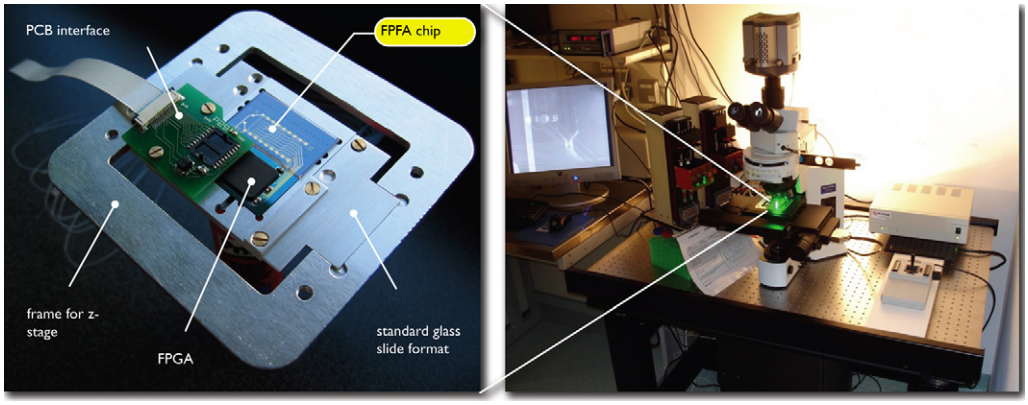

Fig. 1. Left image: the modular adapter for FPFAs. Right image: overall setup for laser-induced biomolecule manipulation experiments and generally biochip application using fluorescence detection.

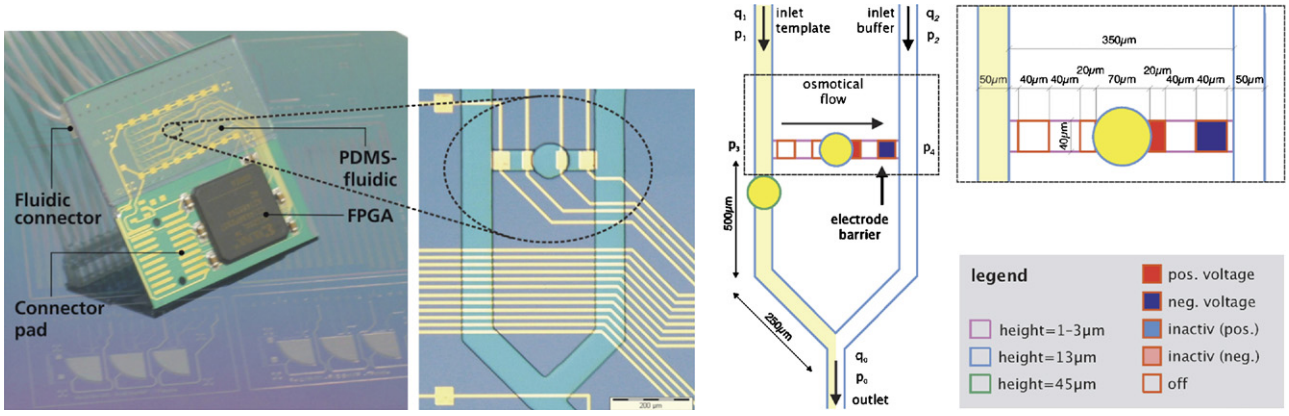

Fig. 2. Left image: full assembled hybrid microfluidic chip with a silicon micromachined electrode layer and micromoulded PDMS fluidics, controlled via a programmable logic device (FPGA); the higher magnification view in the middle shows a microscopic image of the microfluidic "H"-structure containing a circular reaction chamber. The right schematic view clarifies the dimensions of microfluidic channels and chambers as well as the electrodes.

voltage-levels between both extreme values (in the sub-100 kHz range, transmission effects can be neglected). The electrodes, the CCD camera as well as the high performance micropumps were controlled by a conventional PC and a user-friendly custom made software (Fig. 3).

2. Experimental results

To control the transport, pre-concentration and transfer of single-stranded DNA within the system, two different aqueous solutions were injected via Hamilton syringes into both inlets: the first is a freshly prepared histidine buffer solution (50 mM, 73 mS/cm at pH 7.7), the second a diluted solution of Rhodamine-6G-labeled single-stranded DNA oligonuclotides (21 nt, 5×10^{-6} M). To distribute the DNA and buffer solutions into the chip with ultra-low flow rates, the Hamilton syringes were connected to a high-performance microfluidic workstation (Micro Mechatronic Technologies AG). Pump rates were chosen between 1 and 2 μl/h and kept constant in the vertical supply and drain channels.

In order to obtain stable fluid control into and out of the reaction chambers, the pressure driven hydrodynamic flows from the source and the drain channels into the reaction chamber have to be restricted. A single rectangular channel segment contributes the following hydraulic resistances

$$R_{\mathrm{hyd,rect}} = \mathsf{n}\frac{12\eta}{1-0.63(h/w)}\mathsf{g}\frac{L}{h^3 w} = \frac{\Delta p}{q_{\mathrm{hyd}}} \tag{1}$$

where w, h and L is the width, height and length of the channel, respectively, h the viscosity of the fluid and Δp the pressure drop generated by a flow rate q_{hyd}. Note the strong dependence of the channel height $q_{\mathrm{hyd}} \propto h^3$ for a given external pressure drop.

In contrast to this, EOF is described by

$$q_{\mathrm{eof}} = \mathsf{n}\varepsilon\frac{\zeta E}{\eta} wh = v_{\mathrm{eof}} wh, \tag{2}$$

where ε is the permittivity, ζ the zeta potential of the channel wall and E the applied electric field. For a given electroosmotic velocity v_{eof}, the EOF is $q_{\mathrm{eof}} \propto h$. According to $(q_{\mathrm{hyd}}/q_{\mathrm{eof}}) \propto h^2$, a decreased channel height reduces the hydrodynamic flow and hence the EOF dominates the fluid transport. Therefore, a very shallow transfer channel effectively decouples the reaction chamber from hydrodynamic pressure fluctuations inside the microfluidic distribution channels.

The hydraulic resistances of the microfluidic channel system have been calculated and the corresponding network of the setup is shown in Fig. 4. When external syringe pumps are connected to the inlets, generated flow rates $q_1 \neq q_2$ lead to a compensation

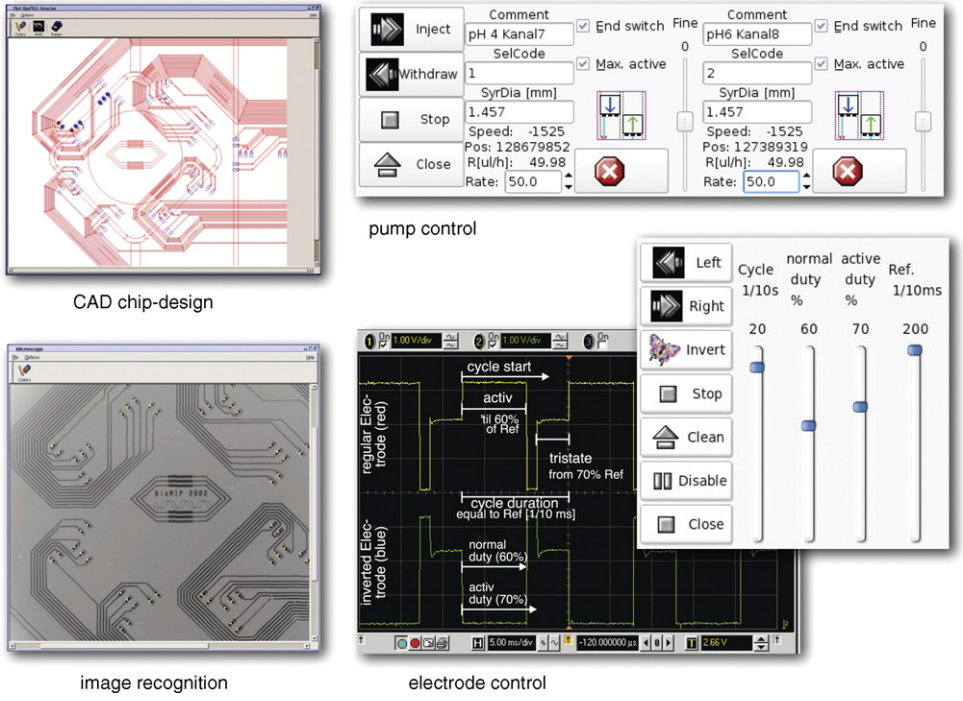

Fig. 3. Control functionalities of the custom made software package.

flow in the horizontal channel. If additionally an electric field is applied, the small gap of 40 μm between the active electrodes acts as an electroosmotic pump producing a flow rate.

According to Kirchoffs law, the net flow and the pressure drop can be calculated and results with the driving EOF-velocity (v_{eof}) along the horizontal channel:

$$v_H = n\frac{r}{wh}\left(q_1\frac{R_3}{R_{eof}} - q_2\frac{R_4}{R_{eof}} + q_{eof}\right) \quad \text{with}$$

$$r = n\frac{R_{eof}}{R_{eof} + R_L + R_3 + R_4}, \tag{3}$$

where r represents a load factor which reduced the ideal EOF.

In Fig. 4, the resulting fluid velocity in the horizontal channels is shown, generated by EOF when:

(a) no external flow is applied ($v_{H,eof}$),
(b) an external asymmetrical flow is applied and the electrodes are switched off ($v_{H,hyd}$) and
(c) both effects are taken into account (v_H).

Furthermore, Fig. 4 demonstrates the effective suppression of the external pressure drop within a shallow channel.

Fig. 5 illustrates the filling procedure of the reaction chamber with a fluorescently labelled DNA solution. The pump rates were adjusted such that a slow Poiseuille flow from right to left

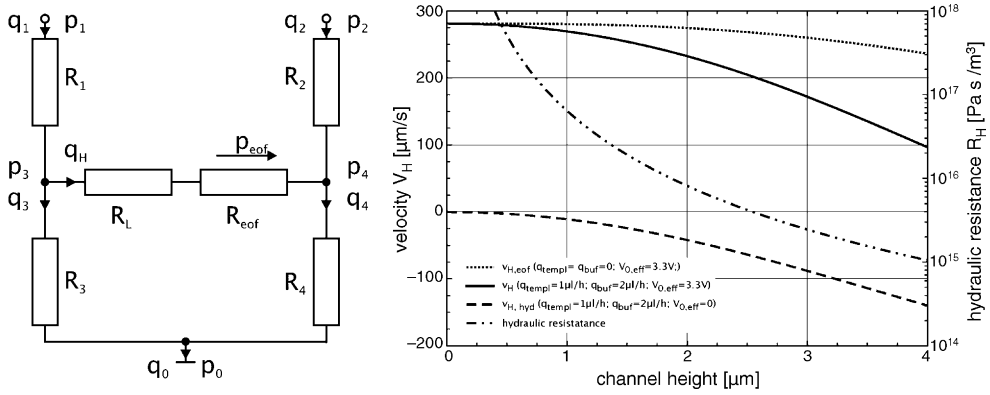

Fig. 4. Left scheme: equivalent network of the hydraulic resistances corresponding to the microchannel arrangement in Fig. 2: (R_1, R_2 are inlet resistances; R_3, R_4 are outlet resistances; R_L is the load resistance and R_{eof} is the resistance of the electroosmotically active part). Since the driving force of an EO pump is the EO velocity, the active segment can be considered as a generator of a pressure drop p_{eof}. The right diagram shows the fluid velocity and hydraulic resistance vs. channel height of the horizontal channel. Calculations were carried out for a load of $r = 0.19$, a field strength of 825 V/cm, a channel width of $w = 40$ μm, an electroosmotic mobility of $m_{eof} = 1.8 \times 10^{-4}$ cm^2/V s and the external flow as given in the legend. The hydraulic resistance of the horizontal channel ($R_H = R_{eof} + R_L$) is drawn at a logarithmic scale.

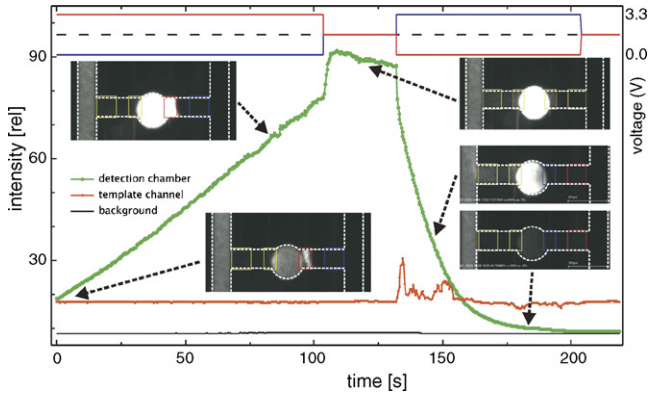

Fig. 5. Fluorescent intensity showing a full cycle of DNA transportation within the detection chamber. This cycle is divided into three parts, indicated by the voltage applied: (i) linear increase of the template concentration; (ii) a linear intensity decrease in absence of any electric field when the detection chamber is washed out slowly by the background (Poiseuille) flow and (iii) a fast reduction of the intensity by inverting the voltage polarity.

in the transfer channel was obtained with no electrodes active. When applying a voltage to a pair of electrodes (as indicated by the red square frame for a positive voltage and a blue square for a zero voltage), an EOF of the fluid solution containing the biomolecules takes place, directed towards the cathode from left to right in the transfer channel.

Simultaneously, negatively charged DNA molecules are repelled by the cathode and migrate back towards the anode, due to the second field effect, electrophoresis. The electrophoretic migration velocity is described by the following equation

$$v_{ep} = \mu_{ep} E \tag{4}$$

where μ_{ep} is the electrophoretic mobility of the DNA oligonucleotides. As long as $v_{ep} > v_{eof}$, the electrode pairs act as ideal barriers regarding the negatively charged biomolecules, resulting in a linear increase of the fluorescence intensity in the detection chamber. No electrolysis was observed up to 200 s. Immediately after enabling the electrodes (tristate, high-impedance), the marginal background flow washes the material from the formerly positive electrode back into the detection chamber and finally into the left feeding channel of the "H"-structure (see also the inset picture of Fig. 5). Because of the considerable difference in transport capacity of the input/output channels and the storage capacity of the reaction/detection chamber, this process is pretty slow. With an appropriate presetting of the electrode potentials, even this slow dilution can be prevented.

The third part in Fig. 5 was to drain the circular reaction chamber again. Two possible draining directions are available: by pumping the material against the background flow into the drain channel, the left pair of electrodes is activated (data not shown). In the case presented here, DNA molecules are moved back into the supply channel, just by an inverted polarity applied to the pair of electrodes formerly used. The two physical effects, reversed EOF and repelling Coulomb force, displace the DNA molecules out of the detection chamber (rapidly, considering the huge size of the reaction chamber in comparison to the shallow input/output channels) in seconds.

3. Conclusions

We have developed a simple microfluidic element based on EOF-driven "artificial membranes". These devices open up new horizons, e.g. for controlled dosing of catalytic/initiator chemicals inside microreactors in order to "switch-on" chemical reactions, specific concentration of molecules at detection spots, separation and/or mixing of reactants in microfluidic biochips as well as on-chip vesicle manipulation (retention and release) by digitally pulsed fields for nano-container-chemistry applications [4].

Acknowledgements

This work was conducted as part of the European Union integrated project PACE (EU-IST-FP6-FET-002035). Mask design and microfabrication by Martina Juenger and Thomas Palutke is greatly appreciated.

References

[1] P.F. Wagler, U. Tangen, T. Maeke, H.P. Mathis, J.S. McCaskill, Microfabrication of a BioModule composed of microfluidics and digitally controlled microelectrodes for processing biomolecules, Smart Mater. Struct. 12 (2003) 757–762.

[2] P.F. Wagler, U. Tangen, T. Maeke, S. Chemnitz, M. Juenger, J.S. McCaskill, in: V.K. Varadan (Ed.), Smart Structures and Materials 2004: Smart Electronics, MEMS, BioMEMS, and Nanotechnology, vol. 5389, Proceedings of SPIE, San Diego, 2004, pp. 298–305.

[3] U. Tangen, P.F. Wagler, S. Chemnitz, G. Goranovic, T. Maeke, J.S. McCaskill, An electronically controlled microfluidics approach towards artificial cells, Complexus 3 (1–3) (2006) 48–57.

[4] P.F. Wagler, U. Tangen, M. Heymann, T. Maeke, S. Chemnitz, M. Juenger, T. Palutke, J.S. McCaskill, The Ninth International Conference on Miniaturized Systems for Chemistry and Life Sciences (μTAS 2005), Boston, 2005, pp. 1134–1136.